The Role of Lysine 529, a Conserved Residue of the Acyl-Adenylate-Forming Enzyme Superfamily, in Firefly Luciferase†

Bruce R. Branchini,* Martha H. Murtiashaw, Rachelle A. Magyar, and Shannon M. Anderson

Department of Chemistry, Connecticut College, New London, Connecticut 06320

Received December 15, 1999; Revised Manuscript Received February 22, 2000

ABSTRACT: Firefly luciferase catalyzes the highly efficient emission of yellow−green light from the substrates luciferin, Mg-ATP, and oxygen in a two-step process. The enzyme first catalyzes the adenylation of the carboxylate substrate luciferin with Mg-ATP followed by the oxidation of the acyl-adenylate to the light-emitting oxyluciferin product. The beetle luciferases are members of a large family of nonbioluminescent proteins that catalyze reactions of ATP with carboxylate substrates to form acyl-adenylates. Formation of the luciferase−luciferyl−AMP complex is a specific example of the chemistry common to this enzyme family. Site-directed mutants at positions Lys529, Thr343, and His245 were studied to determine the effects of the amino acid changes at these positions on the individual luciferase-catalyzed adenylation and oxidation reactions. The results suggest that Lys529 is a critical residue for effective substrate orientation and that it provides favorable polar interactions important for transition state stabilization leading to efficient adenylate production. These findings as well as those with the Thr343 and His245 mutants are interpreted in the context of the firefly luciferase X-ray structures and computational-based models of the active site.

Bioluminescence is an alluring process in which living organisms convert chemical energy into light. Beginning approximately 50 years ago with the pioneering work of Johns Hopkins University scientists William McElroy, Emil White, and Howard Seliger, basic research mainly focused on the North American firefly *Photinus pyralis* (*1*−*3*) has progressed toward a very good understanding of how light is produced by fireflies. As this century draws to a close, the determination of two firefly luciferase (Luc)[1] crystal structures by Conti, Brick, et al. (*4*, *5*) and new mutagenesis studies should advance an excellent understanding of the key structure−function relationships for the highly efficient (*6*) enzyme-catalyzed emission of light in the firefly. In turn, the prospects are bright for the continued application of firefly bioluminescence to the already impressive list of medical and pharmaceutical methods, including those using the firefly luciferase gene as a reporter of gene expression and regulation (*7*−*9*).

† This work was supported by a grant from the National Science Foundation (MCB 9816898) and by the Hans & Ella McCollum-Vahlteich '21 Endowment. It is dedicated to the memory of Professor Emil H. White.

* To whom correspondence should be addressed at the Department of Chemistry, Connecticut College, 270 Mohegan Ave., New London, CT 06320. Tel.: (860) 439-2479; Fax: (860) 439-2477; E-mail: brbra@conncoll.edu.

[1] Abbreviations: CB, 50 mM Tris-HCl (pH 7.0), 150 mM NaCl, 1 mM EDTA, and 1 mM DTT; CoA, coenzyme A; GST, glutathione-*S*-transferase; 6×His, the appended N-terminal peptide MRGSHHHHHHGS encoded by the vector pQE-30; L, dehydroluciferin; L-AMP, dehydroluciferyl-*O*-adenosine monophosphate; Luc, *Photinus pyralis* luciferase (EC 1.13.12.7); LH_2, D-firefly luciferin; LH_2-AMP, luciferyl-*O*-adenosine monophosphate; PBS (phosphate-buffered saline), 140 mM NaCl, 2.7 mM KCl, 10 mM Na_2HPO_4, 1.8 mM KH_2PO_4 (pH 7.3); PheA, the phenylalanine-activating subunit of gramicidin synthetase 1; WT, wild-type *Photinus pyralis* luciferase.

As indicated in eqs 1−3 and Figure 1, the Luc enzyme functions as a monooxygenase, although it does so without the apparent involvement of a metal or cofactor. By some means, amino acid residues are recruited to promote the addition of molecular oxygen to LH_2-AMP, which is then transformed to an electronically excited-state oxyluciferin molecule (Figure 1) and CO_2, each containing one oxygen atom from molecular oxygen (*1*, *10*). Relaxation of excited-state oxyluciferin to the corresponding ground state is accompanied by the emission of light. A quantum yield of ∼0.9 for this process (*6*) reflects not only an efficient catalytic machinery, but also a highly favorable environment for the radiative decay of an excited state.

$$\text{Luc} + \text{LH}_2 + \text{ATP} \overset{\text{Mg}^{2+}}{\rightleftharpoons} \text{Luc·LH}_2\text{-AMP} + \text{PP}_i \quad (1)$$

$$\text{Luc·LH}_2\text{-AMP} + \text{O}_2 \rightarrow \text{Luc·oxyluciferin*} + \text{AMP} + \text{CO}_2 \quad (2)$$

$$\text{Luc·oxyluciferin*} \rightarrow \text{Luc·oxyluciferin} + h\upsilon \quad (3)$$

$$\text{Luc} + \text{L} + \text{ATP} \overset{\text{Mg}^{2+}}{\rightleftharpoons} \text{Luc·L-AMP} + \text{PP}_i \quad (4)$$

Firefly luciferase also catalyzes the in vitro formation of the adenylate of synthetic dehydroluciferin (L-AMP) (eq 4), which cannot react further and potently inhibits Luc activity (*11*). A report (*12*) that Luc can also mediate the transfer of the AMP moiety from L-AMP to ATP to produce diadenosine tetraphosphate indicates that Luc can also function as a ligase. Additionally, CoA can inhibit this ligase function (*12*) and modulate the usual Luc light emission kinetics (*13*, *14*), although the cofactor is not a required substrate. CoA may stimulate light production by promoting the release of product

10.1021/bi9928804 CCC: $19.00
Published on Web 04/13/2000

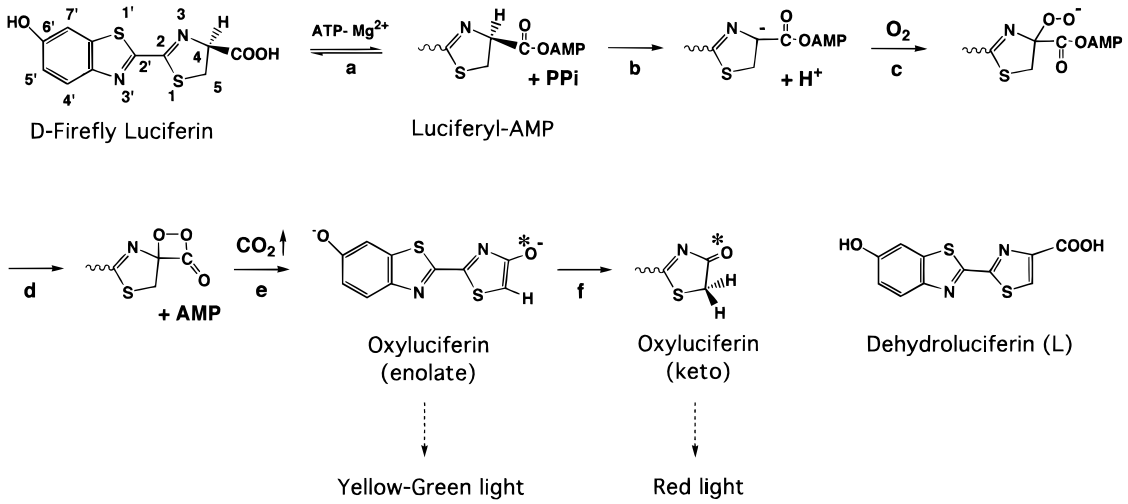

FIGURE 1: Mechanism of Luc-catalyzed bioluminescence and the chemical structure of dehydroluciferin (L).

oxyluciferin (*13*−*15*) and/or by reacting with the Luc·L-AMP complex producing L-CoA and AMP, thereby releasing free Luc (*12*).

The cloning and sequencing of *P. pyralis* luciferase and similar enzymes from 13 other beetle species[2,3] (*16*, *17*) have revealed that these luciferases are closely related to a large family of nonbioluminescent proteins (*18*, *19*) that catalyze reactions of ATP with carboxylate substrates to form acyl-adenylates. The formation of enzyme-bound LH_2-AMP and L-AMP (eqs 1 and 4) illustrates one step of the common chemistry. The "acyl-adenylate/thioester-forming" superfamily of enzymes (*20*) includes the following: a variety of acyl:CoA ligases; the acyl-adenylate-forming domains of enzyme complexes involved in the nonribosomal synthesis of peptides and polyketides (*20*); the luciferases; and several other types of enzymes. Most of these enzymes generate thioester (e.g., of CoA) intermediates or products from the initially formed corresponding acyl-adenylates, and these reactions are similar to one suggested (*12*) to account for the stimulatory effect of CoA on Luc activity.

The Luc crystal structure without bound substrates (*4*), the first structure of a member of the "acyl-adenylate/thioester-forming" enzyme family (*20*), revealed a unique molecular architecture consisting of a large N-terminal domain (residues 1−436) and a small C-terminal domain (residues 440−550). Based on an analysis of the positions of approximately seven strictly conserved residues among a group of enzymes sharing the adenylation function, a general location of the Luc active site was proposed (*4*). Many of these invariant residues were found on the surfaces of the two Luc domains opposite to each other and separated by a wide solvent cleft (*4*). Next, the crystal structure of a second member of the adenylate-forming family, the phenylalanine-activating subunit of gramicidin synthetase 1 (PheA) in a complex with phenylalanine, Mg ion, and AMP, was reported (*21*). The active site of PheA was determined to be at the interface of the two domains, which were remarkably similar in size and shape to the corresponding domains of Luc (*21*). In the PheA structure, however, the C-terminal domain was rotated 94° and was 5 Å closer to the N-terminal domain

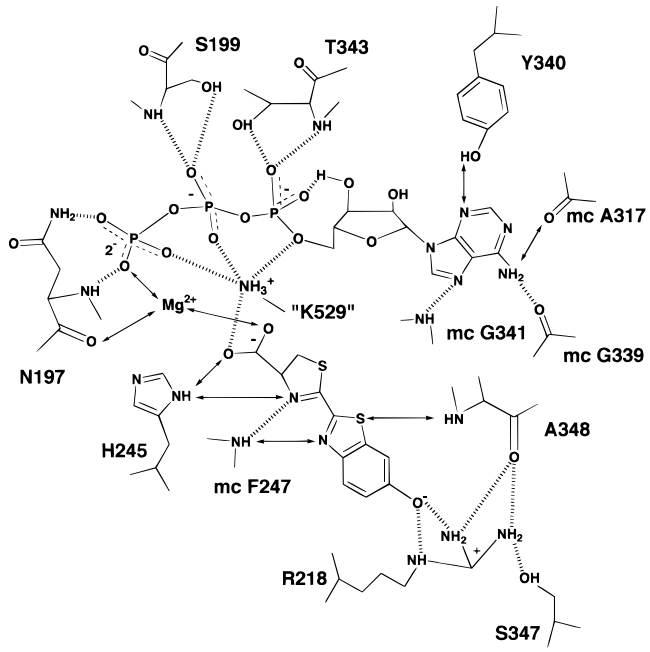

FIGURE 2: Schematic representation of hydrogen bonding (||||) between Luc and substrates LH_2, ATP, and Mg^{2+} predicted by molecular modeling (*22*). Potential interactions between substrates and atoms in close proximity (∼2 to ∼4 Å) are indicated (↔). For main chain (mc) atoms, only those interacting with substrates are included. Methylammonium ion, labeled "K529", was used to represent possible interactions of the Lys529 side chain. For clarity, additional potential contacts of the Mg^{2+} ion with the Thr343 side chain and the O3 atoms of the α- and β-phosphates of ATP are not shown.

than in the "open" Luc structure (*21*). Starting with the crystal structures of Luc (*4*) and PheA (*21*), we used molecular modeling techniques to produce a potential working model (Figure 2) of the Luc active site containing substrates LH_2 and Mg-ATP (*22*). Subsequently, the crystal structure of Luc containing two molecules of bromoform, a general anesthetic and Luc inhibitor, was described (*5*). One of the bromoform molecules binds in a site tentatively identified as the LH_2 binding pocket, based on the location of the phenylalanine binding site in the PheA structure (*5*, *21*). The newly proposed (*5*) Luc site of LH_2 binding is in good general agreement with our proposal (*22*). Moreover, a model of the Luc−ATP−LH_2 complex (*23*) produced by molecular mod-

[2] K. V. Wood and M. Gruber, personal communication.
[3] V. R. Viviani, personal communication.

eling and energy minimization provides an active site description complementary to ours (*22*).

Lys529 is absolutely conserved among at least 40 members of the adenylate-forming superfamily and all of the luciferases. In PheA, electronic interactions between Lys517 (Lys529 in Luc) and both phenylalanine and AMP are believed to fix the C-terminal domain in a productive orientation (*21*). A catalytic role for Lys517 in PheA also has been proposed (*21*) and is generally supported by the results of a mutagenesis study (*24*) on the valine-activating subdomain of surfactin synthetase 1.

In the development of our working model of the Luc active site (*22*), limitations on the size of the searched conformational space did not enable us to include the C-terminal domain. Recognizing the potential importance of Lys529, we included methylammonium ion in our calculations to mimic possible interactions of the side chain ammonium ion (*22*). As illustrated in the schematic diagram (Figure 2), our model predicts that Lys529, along with His245 and Thr343, is proximate to the carboxyl group of substrate LH_2. In a recent mutagenesis study (*25*), we determined that several mutations at residues Thr343 and His245, which also may be near the emitter oxyluciferin, do indeed alter bioluminescence color in Luc. In contrast, two amino acid changes at position 529 did not affect bioluminescence color. We report here the results of new mutational and biochemical studies of Lys529 directed at determining the role of this residue in the beetle luciferases and related enzymes of the adenylate-forming superfamily.

MATERIALS AND METHODS

Materials. The following items were obtained from the indicated sources: Mg-ATP (equine muscle) (Sigma); LH_2 (Biosynth AG); restriction endonucleases, T4 polynucleotide kinase, and T4 DNA ligase (New England Biolabs); and mutagenic oligonucleotides (Genosys). LH_2-AMP was synthesized according to the method of Morton et al. (*26*) and stored at −70 °C as a 0.1 mM solution in 10 mM sodium acetate buffer, pH 4.5, containing 40 mM NaCl. Dehydroluciferin (L) was prepared as described by White et al. (*10*). WT, K529R, and K529Q luciferases containing the additional N-terminal peptide GPLGS- were constructed and purified as GST-fusion proteins as previously reported (*22, 25*).

General Methods. Detailed procedures including descriptions of the equipment used to determine bioluminescence activity of the luciferases by flash height- and integration-based light assays have been described previously (*22, 25*). The procedures, equipment, and methods used to obtain fluorescence emission spectra, steady-state kinetic constants for LH_2 and Mg-ATP, bioluminescence emission spectra, and total protein concentration also have been reported earlier (*22, 25*). The entire cDNA of all luciferase genes was verified by sequencing performed at the DNA Sequencing Facility, Pfizer Inc.

Site-Directed Mutagenesis. To produce the K529A luciferase protein, mutagenesis of WT in the pGex-6P-2 vector was performed with the Chameleon double-stranded mutagenesis kit (Stratagene) using *Alwn*I as the selection endonuclease. Site-directed mutagenesis was carried out according to the manufacturer's instructions using the following primers—5′-GGT CTT ACC GG**T** **GCA** CTC GAC GCA AAG-3′ (*Age*I) and 5′-TCCTGTTACCAGT**C**GC-GA**C**TGCCAGTG-3′ (*Nru*I)—to introduce the K529A mutation and *Alwn*I selection site, respectively (underline represents silent changes to create a unique screening endonuclease site, the boldface type represents the mutated codon, and parentheses indicate the screening endonuclease used).

Cloning, Expression, and Purification of 6×His−Luciferase Fusion Proteins. To produce 6×His versions of the WT, K529Q, and K529R proteins, the corresponding DNA inserts were isolated from the available pGex plasmids by digestion with *Bam*HI and *Pst*I. Each *Bam*HI−*Pst*I fragment was subcloned into the pQE-30 vector (Qiagen) and then transformed with *E. coli* strain BL21 (pREP4).

The 6×His-WT and Lys529 mutant enzymes were overexpressed in BL21 (pREP4) cells. Cultures (250 mL) were grown to mid-log phase (A_{600} = 0.6−0.9) in 1 L flasks at 37 °C in Luria−Bertani medium supplemented with 100 μg/mL ampicillin and 25 μg/mL kanamycin, induced with 0.1 mM IPTG, and incubated at 25 °C for 8−10 h. The cells were harvested by centrifugation at 4 °C and stored overnight at −70 °C. Cell pellets were resuspended in 25 mL of PBS containing 0.1 mM phenylmethylsulfonyl fluoride and 5 mM imidazole. Lysozyme (0.05 volume of 10 mg/mL stock) was added, and the cells were lysed by sonication. The lysate was treated with RNase A (10 μg/mL) and DNase I (5 μg/mL); Triton X-100 (2% final volume) was added; and the whole-cell extract was isolated by centrifugation at 20000*g* for 1 h.

The 6×His-proteins were then purified using Ni−NTA agarose (Qiagen) affinity chromatography. The whole-cell extracts were incubated with Ni−NTA agarose at 4 °C with gentle shaking and packed into 5 mL disposable columns. The Ni−NTA medium was washed with 3−4 column volumes of PBS containing 20 mM imidazole and then eluted with a step gradient (50−500 mM) of imidazole in PBS. Fractions containing 6×His-proteins (250−500 mM imidazole) were pooled, and proteins were isolated by ammonium sulfate fractionation (31−61% of saturated cut taken). Precipitated 6×His-proteins were solubilized in the minimum volume of CB containing 0.4 M ammonium sulfate and 1% glycerol. The protein solutions (0.5−1.5 mL) were then dialyzed overnight against sterile CB containing 0.8 M ammonium sulfate and 2% glycerol (2 changes of 250 mL each). Protein solutions (7−13 mg/mL) were stored at 5 °C for up to 6 months with no loss of activity.

Determination of Dissociation Constants. Dissociation constants (K_d) were determined for substrates LH_2 and Mg-ATP by equilibrium dialysis using a 5-cell equilibrium dialyzer (Spectrum Industries) equipped with Teflon cells (half-cell volume = 0.25 mL). In all studies, Spectrapor 4 dialysis membranes (MWCO = 12 000) separated the half-cells. Solutions (final volume = 0.2 mL) of 6×His-WT, -K529R, and -K529Q luciferases (16−160 μM) in CB containing 0.8 M ammonium sulfate and 2% glycerol were mixed with either Mg-ATP or LH_2 and placed in one side of the dialysis cell. The second dialysis compartment included 0.2 mL of CB containing 0.8 M ammonium sulfate and 2% glycerol. The dialyzer unit was rotated at 10 rpm for 3 h at 21.0 ± 1.0 °C. Under these conditions, the enzymes remained fully active, and the substrates did not deteriorate. For Mg-ATP studies, initial 6×His-enzyme and substrate concentrations were the following: WT, 160 μM, 12−240

μM Mg-ATP; K529Q, 260 μM, 50−500 μM Mg-ATP; and K529R, 40 μM, 15−120 μM Mg-ATP. For studies with LH_2, 6×His-enzyme and substrate concentrations were as follows: WT, 12 μM, 3−30 μM LH_2; K529Q, 100 μM, 15−250 μM LH_2; and K529R, 12 μM, 1.5−30 μM LH_2.

The initial and equilibrium concentrations of substrates used to calculate concentrations of bound and free ligand were quantitated by flash height-based bioluminescence assays (*22*, *25*). For quantitation of LH_2, 10−20 μL aliquots of the initial LH_2 solution cell contents or 20−50 μL aliquots of the equilibrium cell contents were added to 0.4 mL of 25 mM glycylglycine buffer, pH 7.8, containing 0.3 μg of 6×His-WT. Assays were initiated by injection of 0.12 mL of 10 mM Mg-ATP; the final assay volume was 0.52 mL. Mg-ATP was quantitated in a similar manner with light reactions being initiated by injection of 0.12 mL of 0.3 mM LH_2 in 25 mM glycylglycine buffer, pH 7.8. Substrate concentrations were determined from standard curves generated under identical assay conditions with known amounts of LH_2 (0.1−1.5 nmol) or Mg-ATP (0.4−4.0 nmol) added. Linear relationships with regression coefficients of 0.97 and 0.99 were obtained for Mg-ATP and LH_2, respectively. K_d values and the number of binding sites per mole of enzyme were calculated according to the methods described by Lee and McElroy (*27*).

Kinetic Studies with LH_2-AMP. K_m values were obtained from bioluminescence activity assays in which measurements of maximum light intensities were taken as estimates of initial velocities. Into 50 mM Tris buffer, pH 7.1 (0.4 mL) at 25 °C, were added 0.1 mL aliquots of a stock solution of LH_2-AMP in 10 mM sodium acetate buffer, pH 4.5, containing 40 mM NaCl (final concentration of LH_2-AMP 0.25−40 μM). Immediately, light reactions were initiated by injection of luciferase enzymes (2 μg in 10 μL of CB containing 0.8 M ammonium sulfate and 2% glycerol). At the final assay pH of 7.1, the hydrolytic decomposition of LH_2-AMP was negligible for the duration of the assays. Peak height data were collected, and kinetic constants were calculated using the Enz-Fitter (Biosoft) software as previously described (*22*, *25*) except that V_{max} values were expressed in units of einstein $\times 10^{-6}$ s^{-1}. The corresponding k_{cat} values were obtained by dividing the V_{max} values by the final amounts (μmol) of each luciferase in the assay mixtures.

Fluorescence-Based Determination of L Binding and Rate of L-AMP Formation. It has previously been demonstrated (*29*) that the formation of a luciferase−L complex could be monitored by the enhancement of the 440 nm fluorescence emission of L, which is very weak in the absence of enzyme. Using an excitation wavelength of 350 nm, the fluorescence emission spectra (390−650 nm) of 0.4 μM solutions of L in 50 mM Tris buffer, pH 7.4, determined by UV−Vis spectroscopy using $\epsilon_{350} = 22\,100$ M^{-1} cm^{-1} (*28*), were recorded before and after the addition of WT or the mutant luciferases (3.2 μM final concentration). The emissions of L at 440 nm in the presence and absence of each luciferase were compared to assess the formation of an enzyme−L complex (*29*).

It has previously been determined (*28*, *29*) that the luciferase-catalyzed formation of L-AMP from L, initiated by the addition of Mg-ATP (eq 4), could be assessed by following the decrease in the intensity of the 440 nm fluorescence of the initial enzyme−L complex. Measurements of the change in 440 nm fluorescence accompanying L-AMP formation were used to estimate the rates of L-AMP formation catalyzed by the mutant luciferases and WT. In separate trials, the initial fluorescence at 440 nm (excitation at 350 nm) of solutions of each luciferase (1.0 μM) and L (100 μM) in 0.5 mL of 50 mM Tris buffer, pH 7.4, was recorded. The decrease in the 440 nm fluorescence emission was monitored following the rapid injection of 40 μL of solutions of varying concentrations of Mg-ATP in the same buffer. For WT, H245A, and T343A, Mg-ATP was varied over the range of 0.05−0.2 mM, and for the K529 mutants, Mg-ATP was varied over a range of 0.2−3.0 mM. For each enzyme studied, the rates of decrease of the 440 nm fluorescence emission were calculated and used to determine the initial velocities for each Mg-ATP concentration used. The initial velocity data for each enzyme were fitted to a rectangular hyperbola using a nonlinear least-squares method (Enz-Fitter, Biosoft), and the V_{max} values (μmol/s) were obtained by extrapolation of the curves obtained. The corresponding k_{cat} values were obtained by dividing the V_{max} values by the final amount (μmol) of each luciferase in the assay mixtures.

RESULTS

Overexpression, Purification, and Characterization of Luciferase Proteins. WT and the mutant luciferases listed in Table 1 were expressed as GST-fusion proteins and contained the additional N-terminal peptide GPLGS- (*22*, *25*), which remained after protease cleavage of GST. Average yields of purified WT, K529R, K529Q, and K529A were 12, 8, 5, and 3 mg/L of culture volume, respectively. Additionally, 6×His versions of WT, K529R, and K529Q containing the appended N-terminal residues MRGSHHHHHHGS- were expressed and purified by affinity chromatography. The 6×His versions of the WT, K529R, and K529Q enzymes were isolated in improved yields of 34, 30, and 13 mg/L of culture volume, respectively. All proteins were purified to homogeneity as judged by sodium dodecyl sulfate−polyacrylamide gel electrophoresis (data not shown).

The tertiary structure and thermodynamic stability of the Lys529 mutants appeared to be very similar to those of WT as assessed by the protein Trp residue fluorescence emission spectra measured both in the absence and in the presence of 3.5 M guanidinium chloride (data not shown). Previously, we had determined that 3.5 M guanidinium chloride represented the midpoint denaturant concentration for WT and several other single-point Luc mutants (*22*, *25*). Similarly, the thermostability of the K529 mutants, as judged by measurements of activity half-lives at 37 °C, was quite similar (within 10%) to that of WT (data not shown).

Bioluminescence Activity of the Luciferases. Our previously proposed model (*22*) of the Luc active site suggested that only the side-chain groups of His245, Thr343, and Lys529 are within 6 Å of the C4 or C5 atoms of LH_2 (Figure 2). These Luc residues are strictly conserved in the 20 available luciferase sequences[2,3] (*16*, *17*); however, only Lys529, the focus of this study, is absolutely conserved in the adenylate-forming superfamily as well. His245 and Thr343 were shown (*25*) to have significant roles in the determination of bioluminescence color as evidenced by the red-shifted bioluminescence emission maxima associated

Table 1: Bioluminescence Activity of Luciferase Enzymes

enzyme	relative specific activity[a] flash height	relative specific activity[a] integrated	bioluminescence emission maximum[b](nm)	rise time[c] (s ± 0.15)	decay time[d] (min)
WT	100.0	100.0	558 (62)	0.5	0.2
K529R	0.16	1.0	560 (65)	0.6	4.1
K529Q[e]	0.06	7.1	560 (65)	0.7	45
K529A[f]	0.06	13.0	562 (93)	0.6	106
H245A[g]	26.4	80.0	604 (93)	0.9	0.9
T343A[g]	1.1	19.5	617 (65)	1.8	8.9

[a] Specific activity measurements were made as previously described (*22, 25*). WT values are defined as 100.0 and are equivalent to 1.18×10^{15} photons s^{-1} mg^{-1} (0.12 einstein $\times$ 10^{-6} s^{-1} μmol^{-1}) and 2.45×10^{16} photons mg^{-1} (2.5 einstein $\times$ 10^{-6} μmol^{-1}) for flash height-based and 15 min integration-based assays, respectively. Due to the extended decay time for the K529Q and K529A mutants, integrals were recorded for 50 and 110 min, respectively. Light intensity data were corrected for the spectral response of the Hamamatsu 931B photomultiplier tube and differences in the bandwidths of the emission spectra (*22, 25*). The error associated with these measurements is ±10% of the value. [b] Bioluminescence emission spectra were measured as described earlier (*25*). Bandwidths (nm) at 50% of emission maxima are indicated in parentheses. [c] Values determined as previously described (*22, 25*). [d] Bioluminescence decay times (to 20% of initial activity) were measured from maximum initial flash heights. These data are the mean of two measurements with a SD ± 10%. [e] Substrate concentrations in the activity assays were 2 mM Mg-ATP and 0.4 mM luciferin. [f] Substrate concentrations in the activity assays were 3.0 mM Mg-ATP and 0.5 mM luciferin. [g] Data taken from refs *22* and *25*.

with many of the Luc enzymes containing amino acid changes at the corresponding positions (Table 1). In contrast, all of the Lys529 mutants have emission maxima very similar to WT, although the K529A-catalyzed bioluminescence does exhibit greater peak broadening (Table 1).

Specific activities for all luciferases were measured, corrected for differences in the colors and shapes of their emission spectra (*25*), and expressed as flash height- or integration-based values (Table 1). The former values relate the maximum achievable overall reaction rate for the combined adenylation and oxidation steps (eqs 1−3). The relative values presented in Table 1 are comparisons of the mutant enzymes to WT. Among the position 529 mutants, the conservative substitution Lys to Arg resulted in a considerably lower (~625-fold) specific activity for the K529R enzyme compared to WT. The loss of the positively charged side chain was more deleterious, however, as the K529Q and K529A mutants both had ~1650-fold reduced specific activities (Table 1). By comparison, the specific activities of the H245A and T343A mutants lacking the imidazole and hydroxyl side-chain groups at these positions were reduced ~4- and ~90-fold, respectively, compared to WT (Table 1). Although the specific activity of the 6×His-WT was 80% that of WT from the GST-fusion protein, the values for the K529 mutants were the same regardless of the source (data not shown).

The flash height-based specific activities do not take into account the time it takes each enzyme to achieve its maximum light output (i.e., rise time) or the duration of the light emission. These specific activity values, however, are useful for making comparisons of the WT and mutant luciferase properties. The time dependence of bioluminescence intensity of the luciferases varied as the data presented in Table 1 indicate. Particularly, K529Q and K529A enzymes had especially prolonged emission profiles resulting from very slow emission decay rates. Integrated specific activity values (photons/mg) for the luciferases were determined from estimates of the total light output in bioluminescence assays conducted under optimum conditions for each enzyme as specified in Table 1. For the K529Q and K529A proteins, the relative (to WT) integrated values were ~120- and ~220-fold greater than their corresponding flash height-based ones, whereas that of K529R was ~6-fold higher. Unlike WT, all of the mutant luciferase enzymes listed in Table 1 had lower flash height-based specific activities than integration-based values, reflecting their overall slower rates of photon production.

Table 2: Apparent Kinetic Properties and Dissociation Constants of Luciferase Enzymes

enzyme	K_m (μM)[a] luciferin	K_m (μM)[a] Mg-ATP	K_d (μM)[b] luciferin	K_d (μM)[b] Mg-ATP	k_{cat} (s^{-1})[c]
WT	15	160	nd	nd	0.125
6×His-WT	17	158	4.7	169	0.092
K529R[d,e]	16	40	13.2	37	0.0002
K529Q[d,e]	161	829	23.0	1250	0.0001
K529A	230	1200	nd	nd	0.0001
H245A[f]	15	240	nd	nd	0.0406
T343A[f]	99	857	nd	nd	0.0011

[a] Kinetic constants were determined as described (*25*) except that V_{max} values were expressed in units of einstein $\times$ 10^{-6} s^{-1} and the corresponding k_{cat} values were obtained by dividing the V_{max} values by the final amount (μmol) of each luciferase in the assay mixtures. The error associated with K_m values falls within ±10% of the value. [b] Dissociation constants were determined for 6×His-luciferases by equilibrium dialysis as described under Materials and Methods. The error associated with K_d measurements is ±10% of the value. Data not determined (nd). [c] Calculated from the data used to determine the K_m values for LH_2; the error associated with these measurements falls within ±15% of the value. [d] K_m values for LH_2 and Mg-ATP were determined for proteins isolated from GST- and 6×His-constructs and were identical within experimental error. [e] K_d values measured with 6×His-isolated proteins. [f] Data for H245A and T343A taken from refs *22* and *25*.

Effects of Luciferase Mutations on Substrate Binding and Catalytic Constants. To evaluate the effects of substitutions at position 529 on the kinetic behavior of Luc, the steady-state kinetic parameters for the WT and mutant luciferases were determined (Table 2). The conservatively changed K529R luciferase had essentially the same K_m value as WT for LH_2; however, the K_m value for Mg-ATP indicated that it bound this substrate more tightly than WT. Eliminating the positively charged side chain of Lys caused substantial increases in the K_m values for both LH_2 and Mg-ATP (Table 2).

The measured k_{cat} values for all of the Luc mutants reflected the pronounced differences in overall flash height-based specific activities (Tables 1 and 2). The flash height-based values shown in Table 1 and the k_{cat} values in Table 2 are both based on the same maximal rate of the overall reaction (eqs 1−3 and Figure 1). The effects of the changes

Table 3: Apparent Kinetic Properties of Luciferase Enzymes with Synthetic LH_2-AMP[a]

enzyme	k_{cat} (s^{-1})	K_m (μM)	rise time (s ± 0.15)	decay time[b] (min ± 0.01)
WT	0.18	4.7	0.4	0.04
K529R	0.08	4.4	0.5	0.20
K529Q	0.18	5.9	0.5	0.20
K529A	0.09	12.6	0.5	0.12
H245A	0.13	1.7	0.8	0.08
T343A	0.002	0.8	1.2	0.25

[a] Kinetic constants were determined for enzyme-catalyzed bioluminescence reactions initiated with synthetic LH_2-AMP as described under Materials and Methods. The error associated with K_m and k_{cat} values falls within ±10% of the value. [b] Bioluminesence decay times (to 20% of initial activity) were measured from maximum initial flash heights.

Table 4: Estimated Relative Rates of Reactions Catalyzed by Luciferase Enzymes

enzyme	overall rate[a]	adenylation reaction[b]	oxidative reaction[c]
WT	1.0	1.0	1.0
K529R	0.0016	0.002	0.44
K529Q	0.0008	0.006	1.0
K529A	0.0008	0.010	0.50
H245A	0.3248	0.688	0.72
T343A	0.0088	0.125	0.011

[a] Relative overall rates are based on overall k_{cat} values (Table 2) calculated from the bioluminescence activity data used to determine the K_m values for LH_2; the error associated with these measurements falls within ±15% of the value. [b] Relative rates are based on k_{cat} values for enzyme-catalyzed measurements of L-AMP formation from L and Mg-ATP based on fluorescence measurements as described under Materials and Methods. The value for WT was 4.8 s^{-1}, and the error associated with these determinations falls within ±20% of the value. [c] Relative rates are based on k_{cat} values calculated for bioluminescence reactions using synthetic LH_2-AMP (Table 3); the error associated with these measurements falls within ±10% of the value.

at position 529 on k_{cat} were more pronounced than those on K_m (Table 2). The catalytic ability of all of the K529 mutants was significantly compromised as evidenced by k_{cat} values 625-fold (K529R) and 1250-fold (K529Q and K529A) lower than WT. Attempts to chemically "rescue" the activity of the Lys529 mutants by the addition of 20 mM lysine to the activity assays failed to alter the K_m or k_{cat} values of the Lys529 mutants (data not shown).

LH_2 and Mg-ATP Binding Constants. Using equilibrium dialysis methods, the K_d values were obtained for 6×His-WT, -K529R, and -K529Q with substrates LH_2 and Mg-ATP. For the three enzymes studied, the K_d values were very similar to their respective K_m values (Table 2), except that the K_d value of K529Q for LH_2 was 7-fold lower than the corresponding K_m. The K_d values for K529A with Mg-ATP were not measured because the quantities of this enzyme needed to enable the accurate quantitation of free and bound substrate concentrations were not readily available.

An additional qualitative assessment of the integrity of the LH_2 binding sites of the luciferase mutants was made by measuring their ability to enhance the intensity of the 440 nm fluorescence emission of L. This fluorescence change is associated with the formation of a luciferase−dehydroluciferin complex (*29*). With excitation at 350 nm, pH 7.4 solutions of L alone display a very weak emission at 440 nm and an intense band at 550 nm, presumably representing the respective un-ionized and ionized phenolate transitions (*29*). WT and all of the Luc mutants enhanced the 440 nm fluorescence emission band of L ~15-fold (data not shown), while the intensity of the 550 nm peak remained unchanged. These results are very similar to those reported (*29*) for L binding to native *P. pyralis* luciferase. This protein-induced fluorescence enhancement that accompanies enzyme−L complex formation (*29*) is thought to be due to an increase in the quantum yield of the emission of the small fraction of un-ionized (phenol form) L molecules.

Effects of Luciferase Mutations on the Luc Partial Reactions. Measurements of the kinetic properties of WT and the Luc mutants with synthetic LH_2-AMP were undertaken to evaluate the effects of the amino acid changes on the Luc-catalyzed oxidative chemistry (eqs 2 and 3) after and independent of the rate of adenylate formation (eq 1). The light emission profiles (rise and decay times) of all the luciferase mutants with the preformed adenylate were similar (Table 3) to WT. The extended decay times of the Lys529 mutants and T343A that had previously been observed were greatly reduced when LH_2-AMP was substituted for substrates LH_2 and Mg-ATP (Table 2). Using the k_{cat} values for the enzyme-catalyzed production of bioluminescence from LH_2-AMP (Table 3), we estimated the rates of the oxidation reactions (eqs 2 and 3) for the luciferase mutants relative to WT (Table 4). For H245A and T343A, the reduced rates of the oxidation reaction, 1.4-fold and 90-fold, respectively, were similar to the 3.1-fold and 114-fold reduction of the rates of the respective overall reactions. With the K529 mutants, however, the rates of light production from synthetic LH_2-AMP were within a factor of ~2 of the value for WT (Tables 3 and 4). These values for the Lys529 mutants represented dramatically increased rates of light production compared to the overall reactions that were 625- to 1250-fold slower than WT.

The relative rates of the adenylation reactions catalyzed by the luciferases (eq 1) were approximated from estimates of the corresponding rates of formation of the adenylate of synthetic dehydroluciferin (L-AMP) (eq 4). Lacking a proton adjacent to the carbonyl group, L-AMP cannot be oxidized by Luc, and the oxidative steps (eq 2 and 3) do not occur. The rates of enzyme-catalyzed production of L-AMP were estimated by monitoring the decrease in 440 nm fluorescence of solutions of luciferases, L, and Mg-ATP. The basis for this methodology is that enzyme−L complexes display intense 440 nm fluorescence, whereas free L and enzyme-bound L−AMP fluoresce very weakly (*11, 28, 29*). Estimated rates of the adenylation reactions catalyzed by the luciferase mutants, subsequently obtained from k_{cat} values for the formation of L-AMP, are compared to WT in Table 4. The value for the H245A enzyme was approximately the same as WT, while there was an 8-fold decreased adenylation rate with the T343 mutant protein. The Lys529 mutants, however, had 100−500-fold lower adenylation rates compared to the WT enzyme.

DISCUSSION

Interpretation of the Kinetic Results of the Luciferase-Catalyzed Adenylation and Oxidation Reactions. The results of prior mutational and biochemical studies (*25*) enabled us to propose mechanisms for color determination in firefly bioluminescence. An essential role for Thr343, the participa-

tion of His245 and Arg218, and the involvement of bound AMP were postulated. We did not, however, discover any evidence that Lys529, a residue stringently conserved among all luciferases and members of the adenylate-forming family of enzymes, is a determinant of bioluminescence color (*25*). The results of specific activity and overall reaction rate (k_{cat}) measurements (Tables 1 and 2) reported here, however, strongly suggest that Lys529 is of great significance to the overall catalysis of light production (Figure 1). It is possible that the mutations at position 529 affected the individual adenylation (eq 1) and/or oxidation steps (eqs 2 and 3). The complex oxidation process is thought (*1*, *10*) to include the enzyme-assisted removal of a proton at the C-4 position of LH_2 followed by the addition of molecular oxygen at that site, and the subsequent generation of excited-state oxyluciferin from a putative dioxetanone intermediate (Figure 1, steps b through e). Since the k_{cat} values for the overall reactions as well as those with synthetic LH_2-AMP were determined from measurements of emitted light, the efficiency of the formation of product oxyluciferin in its electronically excited state and the efficiency of the radiative decay of the excited-state product also contributed to the calculated rates. This is because the rate of photon production is dependent not only on the rate of oxyluciferin formation but also on the yield of oxyluciferin molecules formed in the electronically excited state and on the efficiency with which the excited-state product decays radiatively.

Using steady-state kinetic measurements, we attempted to estimate the effects of the point mutations on the individual adenylation and oxidation reactions, and these data are presented in Tables 3 and 4. While the Lys529 mutants are the main topic of interest here, the T343A enzyme was also further investigated since prior studies had demonstrated (*25*) the likely catalytic importance of Thr343 and because this residue is part of the highly conserved motif II (*20*) (^{340}YGLTE^{344} in Luc) in the acyl-adenylate-forming enzyme family (*4*). The further evaluation of the H245A mutant was included as a control since we had determined the His245 residue did not have a significant catalytic function (*22*, *25*).

By substituting synthetic LH_2-AMP for LH_2 and Mg-ATP and by monitoring the light emission from bioluminescence reactions catalyzed by WT and the mutant luciferases, we determined the steady-state k_{cat} values for the overall oxidation processes (eqs 2 and 3). Reassuringly, the H245A mutant catalyzed the oxidative steps about as well as WT. The k_{cat} values for the Lys529 mutants with the synthetic adenylate were all within a factor of 2 of WT (Table 3), representing dramatically increased rates of light production and bioluminescence decay rates, compared to reactions with the normal substrates. Moreover, the position 529 mutants displayed similar affinity for the synthetic adenylate (Table 3). These results (Tables 3 and 4) established that it is very unlikely that Lys529 participates substantively in the oxidative steps that include maintaining a favorable environment for excited-state formation and radiative decay. If the C-terminal domain of Luc has an important role in establishing an environment for efficient light emission as has been postulated (*4*), Lys529 is apparently not a residue critical for this function. However, the mutations at position 529 have caused significant reductions in the total bioluminescence yields (Table 1). Possibly, the Lys529 mutations favor the occurrence of a normally minor competing dark reaction. There is evidence for such a dark reaction in a report (*12*) that under certain conditions LH_2-AMP, generated as shown in eq 1, is oxidized by Luc to produce low levels of L-AMP.

The slow decay kinetics of the Lys529 enzymes with the normal substrates may reflect a greatly reduced rate of product inhibition simply because the overall reaction proceeds so slowly. It is known (*1*, *28*) that Luc light emission can be prolonged by using low ATP concentrations ($\leq$micromolar), which presumably effect decreased rates of product release. Moreover, the rapid flash kinetics observed with the Lys529 mutants and LH_2-AMP seem to indicate that the significant role of Lys529 is in the adenylation chemistry. In contrast to the results obtained with the other mutants, the T343A enzyme had a 90-fold lower k_{cat} value for the oxidative steps. Since the overall reaction rate had similarly decreased approximately 110-fold, it appears that Thr343 does participate significantly in the oxidative chemistry and/or processes related to excited-state formation and decay. This result is consistent also with our previous finding (*25*) that Thr343 has an important role in bioluminescence color determination and the normal processes related to excited-state formation and decay.

The estimated relative rate of adenylation with the H245A mutant (Table 4), as anticipated, suggested that His245 is not important for the catalysis of the adenylation partial reaction. Thus, the elimination of the imidazole side chain group at position 245 had little effect on either the adenylation or the oxidation reactions, a result consistent with the minor decrease observed in the overall reaction rate (Table 4). The T343A mutation resulted in an 8-fold lower adenylation rate, suggesting that Thr343 may be important to both partial reactions. The decrease in the rate of the overall oxidative reaction, however, was more than an order of magnitude greater than that of the adenylation rate and approximately equal to the decrease in the overall reaction process. The $\sim$100- to $\sim$170-fold reductions in the adenylation rates with K529A and K529Q were approximately an order of magnitude less than the reductions in the overall reaction rates, while the 500-fold reduction for the K529R enzyme is approximately equal to the decrease in the overall reaction rate. We believe these kinetic results indicate that Lys529 is very important to the catalysis of acyl-adenylate formation, but much less so to the oxidative process.

Proposed Roles of K529 and Thr343 in Luc Bioluminescence. Our model of the Luc active site (Figure 2) predicted (*22*) that Lys529 in WT makes an ion pair interaction with the carboxylate of LH_2 and forms hydrogen bonds to the ribose O-5′ and both the β- and γ-phosphates of ATP (*22*). In the crystal structure of PheA, the ammonium ion of Lys517 makes an ion pair interaction with the carboxylate of substrate Phe and is hydrogen bonded to the ribose O-4′ and O-5′ of product AMP (*21*). Similar interactions are thought to fix the positions of the substrates Phe and ATP at the active site and to maintain the productive orientation of the C-terminal domain (*21*). The deleterious effects on the K_m values for both LH_2 and ATP (Table 2) observed with the K529Q and K529A enzymes, but not with the K529R mutant, provide supportive evidence that the cationic side-chain group of Lys529 assists in the orientation of both the carboxylate substrate and ATP in Luc and the acyl-adenylate-forming family of enzymes. The experimental evidence provided here by the mutagenesis studies of Lys529

supports the premise (*4*, *21*) that a large relative domain movement accompanies substrate binding in Luc.

Additionally, a catalytic role for Lys529 in stabilizing the pentavalent transition state formed during the adenylation process has been proposed (*21*). In a related mutagenesis study, changing the equivalent Lys to Gln (K945Q) in another acyl-adenylate-forming enzyme, the valine-activating subdomain of surfactin synthetase 1, reduced the valine-dependent ATP/PP_i exchange activity by 94% (*24*). The PheA crystal structure (*21*) and the surfactin mutational results (*24*), along with the kinetic results on the Luc partial reactions reported here, strongly support the proposal that the highly conserved lysine residue has an important functional role mainly in the adenylation process. Further, we believe the kinetic data presented here for the K529A and K529Q mutants, both lacking a side chain cationic group, also support the notion that Lys529 makes favorable polar interactions that provide transition-state stabilization leading to efficient adenylate production. We note the apparently contradictory failure of the guanidinium side chain of the K529R mutant to likewise provide transition-state stabilization, thereby resulting in a reduced rate of adenylation (Table 4) with this enzyme. Possibly, this is because the Arg residue at position 529 forms additional and/or preferentially stronger interactions with substrate ATP, as suggested by the 4-fold lower K_m value of the mutant compared to WT (Table 2).

Our model (Figure 2) also suggests that both the main-chain NH and side-chain OH groups of Thr343 form hydrogen bonds to the α-phosphate of ATP. Identical interactions between the equivalent residue (Thr326) and AMP are observed in the crystal structure of PheA (*21*). The results reported here (Tables 3 and 4) suggest that Thr343 participates in both Luc partial reactions and is involved in the binding of LH_2 and Mg-ATP. Thr343 is part of the highly conserved motif II (*20*) (^{340}YGLTE^{344} in Luc) in the acyl-adenylate-forming enzyme family (*4*). The adjacent residue Glu306 (Glu344 in Luc) of 4-chlorobenzoate:coenzyme A ligase has been investigated by mutagenesis and kinetic studies (*20*), and the authors suggested that motif II participates in acyl-adenylate formation and possibly in binding the carboxylate substrate (*20*). It is particularly interesting that the X-ray data (*4*, *5*) suggest a hydrogen-bonding interaction between Glu344 and Ser198 resulting in the spatial association of the signature sequence (motif I, ^{198}SSGSTGLPKG^{207} in Luc) and motif II. In the Luc structure (*4*), these motifs form loops on the surface of the N-terminal domain facing the C-terminal domain across a cleft. We had previously shown (*30*) that Ser198 in Luc is an important determinant of the overall reaction pH optimum and is probably associated with Mg-ATP binding. We believe our present results support the suggestion that motif II is involved in the catalysis of acyl-adenylate formation in the superfamily of adenylating enzymes. Further, we speculate that the residues equivalent to Thr343 in Luc participate in orientating ATP for reaction with the various carboxylate substrates of the adenylate-forming enzymes and perhaps assist Lys529 in the stabilization of the key pentavalent transition state of the adenylation step.

ACKNOWLEDGMENT

We thank Monika Gruber for helpful discussions; David Lloyd, John Thompson, and the DNA Sequencing Facility, Pfizer Inc., for providing the DNA sequencing data; and Lisa Helgerson and Evelyn Bamford for technical assistance.

REFERENCES

1. DeLuca, M. (1976) *Adv. Enzymol. Relat. Areas Mol. Biol. 44*, 37−68.
2. Wood, K. V. (1995) *Photochem. Photobiol. 62*, 662−673.
3. Wilson, T., and Hastings, J. W. (1998) *Annu. Rev. Cell. Dev. Biol. 14*, 197−230.
4. Conti, E., Franks, N. P., and Brick, P. (1996) *Structure 4*, 287−298.
5. Franks, N. P., Jenkins, A., Conti, E., Lieb, W. R., and Brick, P. (1998*) Biophys. J. 75*, 2205−2211
6. Seliger, H. H., and McElroy, W. D. (1960) *Arch. Biochem. Biophys. 88*, 136−141.
7. Campbell, A. K., and Sala-Newby, G. B. (1993) in *Fluorescent and Luminescent Probes for Biological Activity* (Mason, W. T., Ed.) pp 58−82, Academic Press, London.
8. Kricka, L. J. (1995) *Anal. Chem. 67*, 499R−502R.
9. Price, R. L., Squirrell, D. J., and Murphy, M. J. (1998) *J. Clin. Ligand Assay 21*, 349−357.
10. White, E. H., Rapaport, E., Seliger, H. H., and McElroy, W. D. (1971) *Bioorg. Chem. 1*, 92−122.
11. Rhodes, W. C., and McElroy, W. D. (1958) *J. Biol. Chem. 233*, 1528−1537.
12. Fontes, R., Ortiz, B., de Diego, A., Sillero, A., and Günther Sillero, M. A. (1998) *FEBS Lett. 438*, 190−194.
13. Airth, R. L., Rhodes, W. C., and McElroy, W. D. (1958) *Biochim. Biophys. Acta 27*, 519−532.
14. Pazzagli, M., Devine, J. H., Peterson, D. O., and Baldwin, T. O. (1992) *Anal. Biochem. 204*, 315−323.
15. Ford, S. R., Buck, L. M., and Leach, F. R. (1995) *Biochim. Biophys. Acta 1252*, 180−184.
16. Wood, K. V., Lam, Y. A., Seliger, H. H., and McElroy, W. D. (1989) *Science 244*, 700−702.
17. Ye, L., Buck, L. M., Schaeffer, H. J., and Leach, F. R. (1997) *Biochim. Biophys. Acta 1339*, 39−52.
18. Suzuki, H., Kawarabayasi, Y., Kondo, J., Abe, T., Nishikawa, K., Kimura, S., Hashimoto, T., and Yamamoto, T. (1990) *J. Biol. Chem. 265*, 8681−8685.
19. Babbitt, P. C., Kenyon, G. L., Martin, B. M., Charest, H., Sylvestre, M., Scholten, J. D., Chang, K.-H., Liang, P.-H., and Dunaway-Mariano, D. (1992) *Biochemistry 31*, 5594−5604.
20. Chang, K.-H., Xiang, H., and Dunaway-Mariano, D. (1997) *Biochemistry 36*, 15650−15659.
21. Conti, E., Stachelhaus, T., Marahiel, M. A., and Brick, P. (1997) *EMBO J. 16*, 4174−4183.
22. Branchini, B. R., Magyar, R. A., Murtiashaw, M. H., Anderson, S. M., and Zimmer, M. (1998) *Biochemistry 37*, 15311−15319.
23. Ugarova, N. N., and Sandalova, T. P. (1999) in *Bioluminescence and Chemiluminescence—Perspectives for the 21st Century* (Roda, A., Pazzagli, M., Kricka, L. J., and Stanley, P. E., Eds.) pp 437−443, John Wiley and Sons, Chichester, U.K.
24. Hamoen, L. W., Eshuis, H., Jongbloed, J., Venema, G., and van Sinderen, D. (1995) *Mol. Microbiol. 15*, 55−63.
25. Branchini, B. R., Magyar, R. A., Murtiashaw, M. H., Anderson, S. M., Helgerson, L. C., and Zimmer, M. (1999) *Biochemistry 38*, 13223−13230.
26. Morton, R. A., Hopkins, T. A., and Seliger, H. H. (1969) *Biochemistry 8*, 1598−1607.
27. Lee, R., Denburg, J. L., and McElroy, W. D. (1970) *Arch. Biochem. Biophys 141*, 38−52.
28. DeLuca, M., and McElroy, W. D. (1974) *Biochemistry 13*, 921−925.
29. Denburg, J. L., Lee, R. T., and McElroy, W. D. (1969) *Arch. Biochem. Biophys. 131*, 381−391.
30. Thompson, J. F., Geoghegan, K. F., Lloyd, D. B., Lanzetti, A. J., Magyar, R. A., Anderson, S. M., and Branchini, B. R. (1997) *J. Biol. Chem. 272*, 18766−18771.

BI9928804